DEEP LEARNING STUDY FOR IMAGE CLASSIFICATION OF ALZHEIMER'S MRI

Simone Castelli

cstsmn.job@gmail.com

20 May 2025

Abstract

Alzheimer’s disease is a leading cause of dementia, impacting millions worldwide. Early diagnosis is crucial for improving patient outcomes, yet traditional methods often lack the sensitivity to detect early-stage neurodegeneration. This study investigates the application of deep learning models for the classification of Alzheimer’s disease using MRI scans. The research follows the CRISP-DM framework and utilises the "Alzheimer MRI Disease Classification Dataset" from Kaggle, comprising 5,120 MRI images categorised into four classes. To enhance classification performance, the dataset was transformed into a binary classification problem—distinguishing between "No Alzheimer" and "Early Alzheimer" cases—while addressing class imbalance through oversampling techniques. Five deep learning architectures were implemented and compared: Convolutional Neural Networks (CNN), Artificial Neural Networks (ANN), Residual Networks (ResNet50), Visual Geometry Group Network (VGGNet16), and Vision Transformers (ViT). The models were trained and evaluated based on accuracy, precision, recall, and F1-score. Results indicate that CNN achieved the highest accuracy (93.46%), followed by ANN (90.10%) and ViT (86.23%), demonstrating their effectiveness in automated MRI-based Alzheimer’s detection. Future work includes refining model interpretability through explainable AI techniques and integrating larger datasets for improved generalisation. This research highlights the potential of deep learning in advancing early Alzheimer’s diagnosis and supporting clinical decision-making.

Acknowledgements

I would like to express my sincere gratitude to Terri Hoare for her invaluable guidance, encouragement, and constructive feedback throughout this research. Her expertise and support were instrumental in shaping the direction of this study and overcoming the challenges encountered.

I also acknowledge the contributors of the Alzheimer MRI Disease Classification Dataset available on Kaggle, whose efforts in making medical imaging datasets publicly accessible have significantly contributed to advancements in machine learning and medical research.

Lastly, I express my gratitude to the broader academic and research community for their valuable studies and insights, which laid the foundation for this work. This research is dedicated to those affected by Alzheimer's disease, with the hope that technological advancements in artificial intelligence and medical imaging will aid in early diagnosis and improved patient care.

Contents

List of Figures

1. Introduction

Alzheimer's disease is a progressive neurodegenerative disorder that severely impacts memory, cognitive function, and overall well-being. As the primary cause of dementia worldwide, it imposes significant social and economic burdens on individuals and healthcare systems. The World Health Organisation (WHO, 2023) estimates that over 55 million people suffer from dementia globally, with Alzheimer's accounting for 60–70% of cases. Early diagnosis is crucial, as timely intervention can slow disease progression and improve patient outcomes. Recent advancements in artificial intelligence (AI) and medical imaging have opened new possibilities for early detection. Magnetic Resonance Imaging (MRI) is a valuable tool for identifying structural brain changes linked to Alzheimer's. McRobbie et al. (McRobbie, D.W., Moore, E.A., Graves, M.J., & Prince M.R., 2017) emphasise MRI's ability to capture detailed anatomical features, aiding in the identification of early neurodegenerative markers. These innovations align with precision medicine, which tailors' healthcare based on individual differences. This study leverages AI within the CRISP-DM (Cross-Industry Standard Process for Data Mining) framework to classify Alzheimer's stages using MRI scans. Machine learning models analyse the "Alzheimer MRI Disease Classification Dataset" by BorhaniTrash (BorhaniTrash, 2021) from Kaggle, distinguishing between different disease stages.

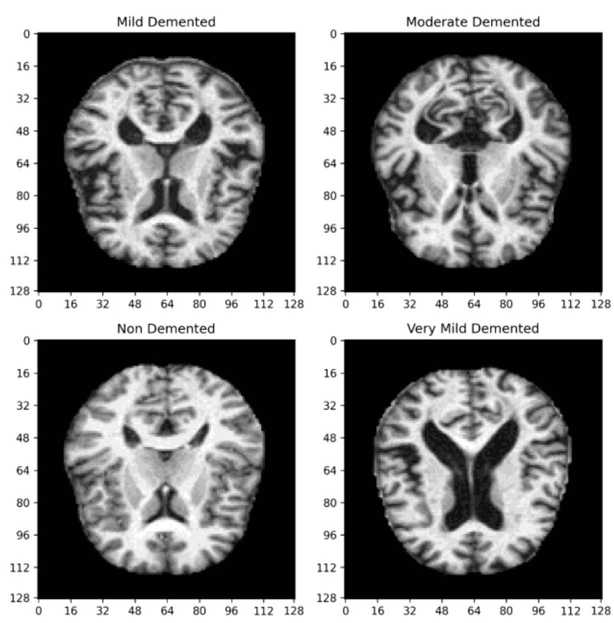

Figure 1: MRI classification categories.

Figure 1 presents MRI scans categorised into four groups: Non-Demented, Very Mild Demented, Mild Demented, and Moderate Demented. By integrating AI and MRI data, this research aims to improve diagnostic accuracy and advance Alzheimer's disease management.

2. Business Understanding

Alzheimer’s diagnosis often relies on cognitive tests, but early detection remains a significant challenge. Magnetic Resonance Imaging (MRI) offers detailed insights into structural changes in the brain, providing a valuable tool for identifying Alzheimer’s at its early stages. However, interpreting these complex images demands advanced computational methods. Deep learning models, such as Convolutional Neural Networks (CNNs), Artificial Neural Networks (ANNs), Residual Networks (ResNet50), Visual Geometry Group Networks (VGGNet16), and Vision Transformers (ViT), have demonstrated great potential in automating the analysis of MRI data. These models excel at detecting subtle structural changes that might be imperceptible to human radiologists. Figure 2 presents MRI sample images of the dataset labelled as ‘Very Mild Demented,’ ‘Mild Demented,’ and ‘Non Demented,’ illustrating the kind of nuanced differences.

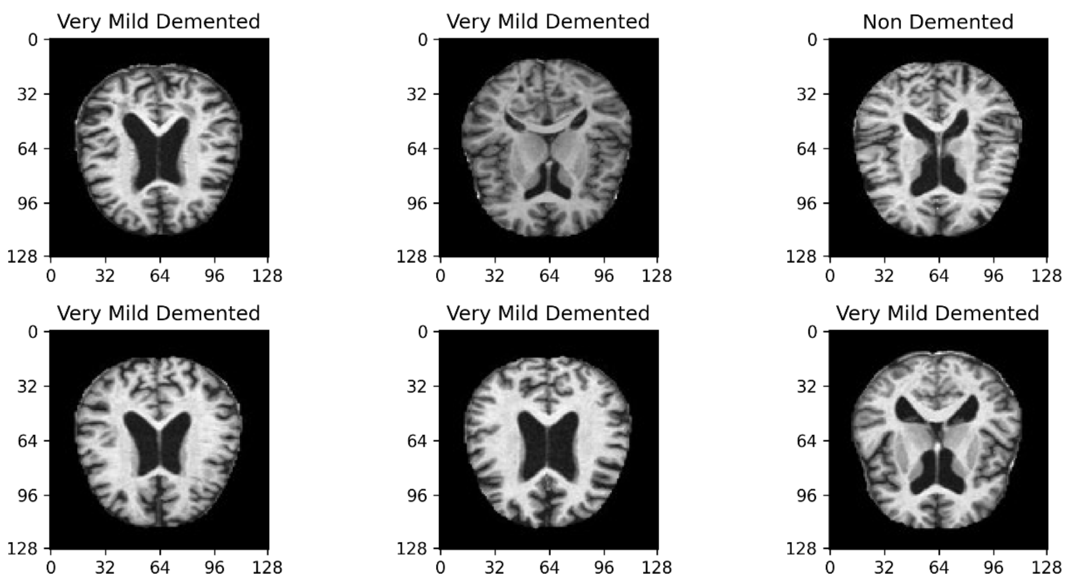

Figure 2: Sample MRI images with labels.

The application of these models is pivotal to achieving key business objectives, such as early diagnosis for timely treatment, reducing the workload for radiologists, and enabling scalable Alzheimer’s screening solutions in resource-constrained environments. By leveraging these state-of-the-art AI techniques, healthcare systems can improve diagnostic accuracy, enhance accessibility, and adopt a more proactive approach to combating the progression of Alzheimer’s disease.

3. Data Understanding

The dataset utilised in this study is the "Alzheimer MRI Disease Classification Dataset," provided by BorhaniTrash (BorhaniTrash, 2021) on Kaggle. This dataset comprises 5,120 grayscale MRI images, each with a resolution of 128x128 pixels, categorised into four distinct classes: Non-Demented, Very Mild Demented, Mild Demented, and Moderate Demented.

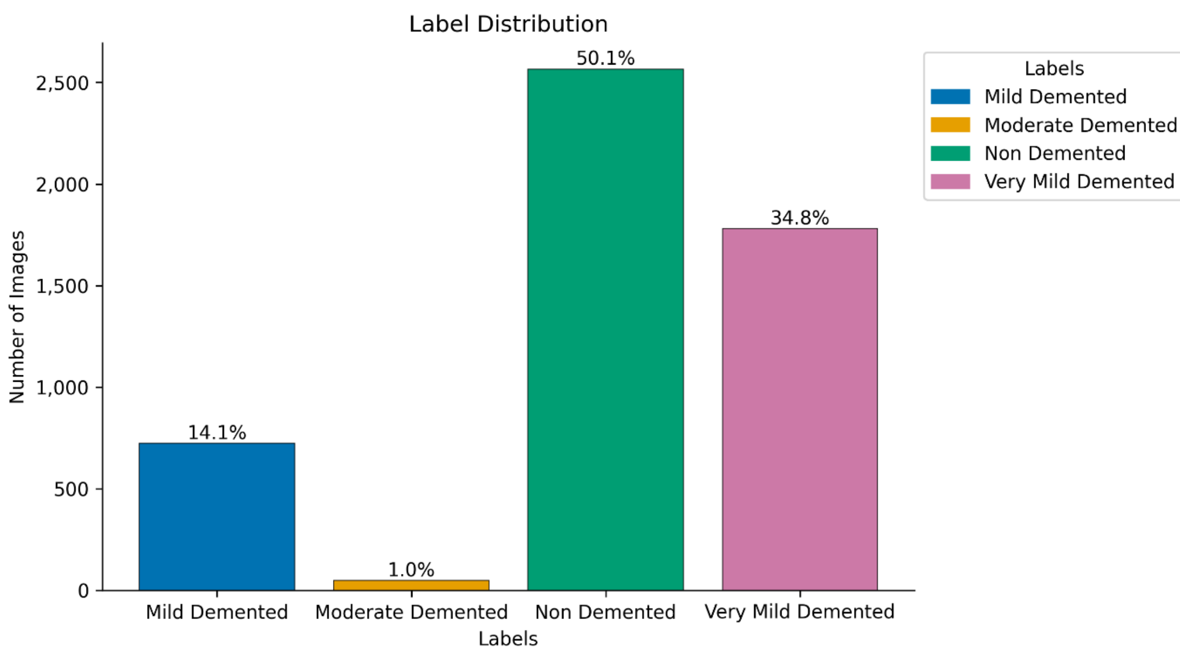

Figure 3: Dataset label distribution.

A critical observation of the dataset, visualised in Fig. 3, reveals an imbalance in class distribution. Specifically, 50.1% of the dataset is Non Demented images, 34.8% represent Very Mild Demented, 14.1% correspond to Mild Demented, and a mere 1.0% consist of Moderate Demented cases. This distribution poses challenges for training models effectively due to the minority representation of the latter two categories.

4. Data Preparation

To simplify the analysis and improve classification focus, the four original labels were consolidated into two binary classes: "No Alzheimer" (0) and "Early Alzheimer" (1). This transformation allows the study to concentrate on distinguishing between healthy individuals and those in the early stages of Alzheimer's disease.

Following this consolidation, the binary label distribution is illustrated in Fig. 4, where the dataset retains near balance, with "No Alzheimer" comprising 50.1% and "Early Alzheimer" making up 49.9% of the images.

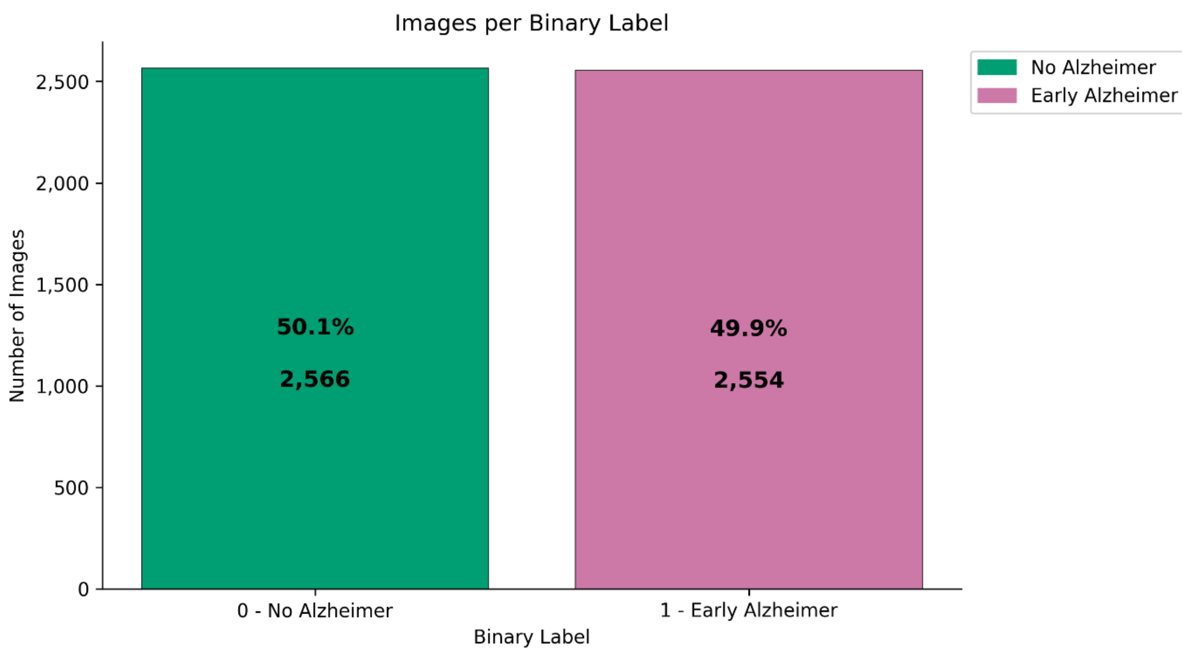

Figure 4: Binary label distribution.

The dataset was partitioned into three subsets: training (60%), validation (20%), and testing (20%), aligning with the recommendations in Ng (Ng, 2018). Stratified sampling was employed to ensure that the proportions of binary labels were maintained consistently across these splits. To address the inherent class imbalance in the training set, oversampling techniques were applied, resulting in a perfectly balanced training dataset.

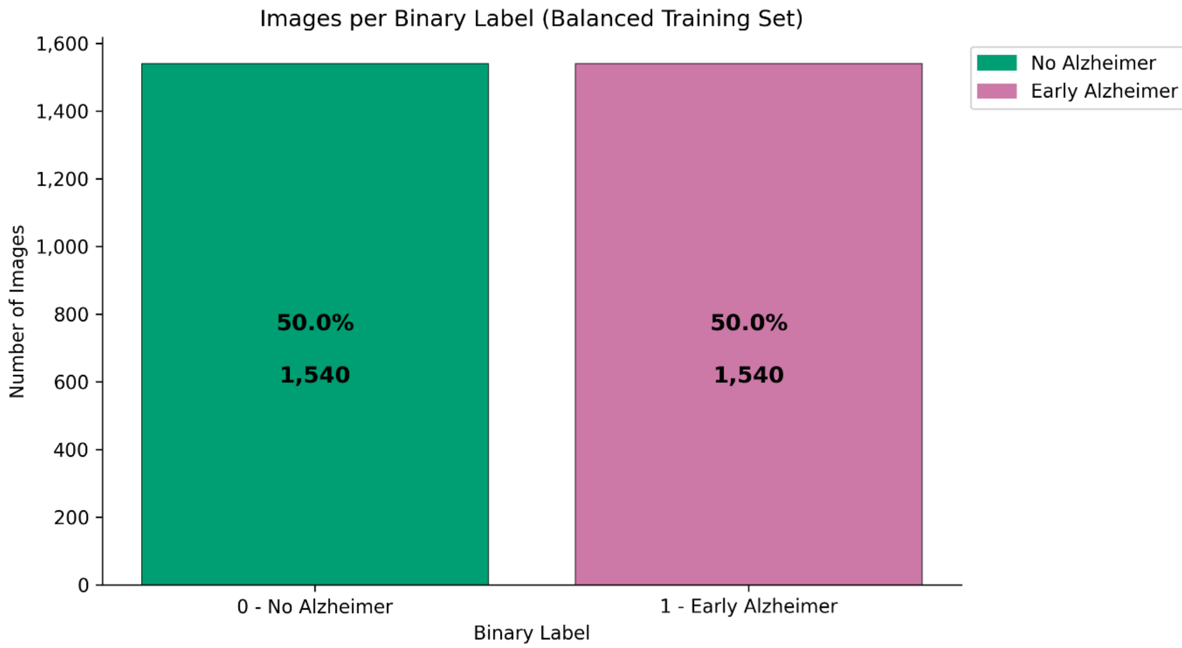

Figure 5: Balanced training set after oversampling.

As depicted in Fig. 5, the oversampled training set contains an equal number of images (1,540) for each binary label, effectively mitigating bias and enabling robust model training. This preparation step was critical in creating a dataset structure conducive to effective learning and evaluation.

5. Modelling

The modelling phase of the CRISP-DM process focuses on classifying MRI scans into 'No Alzheimer' and 'Early Alzheimer' categories. The models employed are Convolutional Neural Networks (CNN), Artificial Neural Networks (ANN), Residual Networks (ResNet50), Visual Geometry Group Network (VGGNet16), and Vision Transformers (ViT). These models were selected for their proven ability to handle complex image data and extract intricate features critical for Alzheimer's diagnosis. CNNs and ANNs are foundational deep learning methods for image classification, offering robust performance in detecting subtle structural changes. ResNet50 and VGGNet16, with their advanced architectures, excel at identifying nuanced patterns in medical imaging. Vision Transformers (ViT) were included to leverage their capability in capturing long-range dependencies and global image features, making them particularly suited for high-resolution MRI analysis. Each model is described in terms of its architecture, data preprocessing, and training procedures.

5.1 Overview of Data Preprocessing

The MRI scans underwent consistent preprocessing to ensure comparability and enhance model performance. Pixel values were normalised to the range [0, 1], promoting faster convergence during training. Single-channel grayscale images were reshaped into three channels to ensure compatibility with models like ResNet50 and VGGNet16. These standardised preprocessing steps established a robust and uniform dataset, enabling fair comparisons across all models. This approach adhered to best practices, ensuring that differences in model performance could be attributed to the models themselves rather than inconsistencies in data preparation.

5.2 Convolutional Neural Networks

Convolutional Neural Networks are specialised neural networks designed for processing structured grid data, such as images, by exploiting spatial hierarchies through local connections and shared weights. A typical CNN architecture comprises multiple layers, including convolutional layers that apply filters to capture local features, pooling layers for dimensionality reduction, and fully connected layers that integrate these features for classification tasks. For instance, in image classification, CNNs can effectively identify patterns like edges, textures, and shapes, leading to accurate object recognition. The training process involves optimising the network's parameters using algorithms like stochastic gradient descent, often with backpropagation, to minimise a loss function that quantifies the difference between the predicted and actual outputs. Regularisation techniques, such as dropout and weight decay, are commonly employed to prevent overfitting and enhance the model's generalisation capabilities. For a comprehensive understanding of CNNs, including their theoretical foundations and practical applications, refer to Goodfellow et al., *Deep Learning* (Goodfellow, I., Bengio, Y., and Courville, A. , 2016).

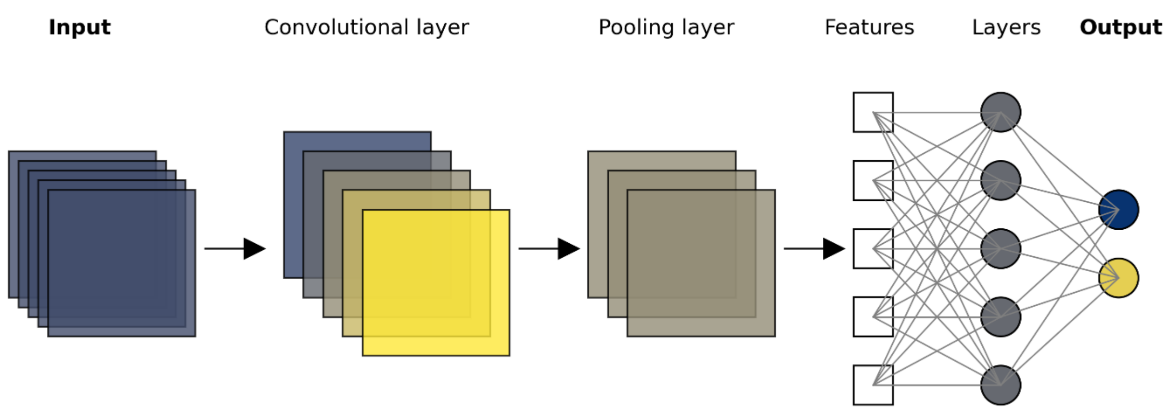

Figure 6: CNN diagram (Author's own).

This diagram illustrates the sequential flow of data through the various layers of a CNN, highlighting the transformation and abstraction of features leading to the final classification output.

5.3 Artificial Neural Networks

Artificial Neural Networks are computational models inspired by the human brain's interconnected neuron structure, designed to recognise complex patterns within data. In this study, the ANN architecture comprises an input layer, two fully connected hidden layers utilising Rectified Linear Unit (ReLU) activation functions to capture non-linear relationships, and an output layer with a sigmoid activation function for binary classification tasks. To prevent overfitting, dropout layers are incorporated during training, randomly omitting a fraction of neurons to enhance the model's generalisation capabilities. The input data undergoes normalisation through standard scaling, ensuring uniform feature distribution, which facilitates efficient learning. The model is trained using the binary cross-entropy loss function alongside the Adam optimiser, selected for its adaptive learning rate and computational efficiency. Early stopping is implemented to monitor the validation loss, ceasing training if no improvement is observed over a set number of epochs, thereby preventing overfitting and conserving computational resources. For a comprehensive understanding of ANNs and their applications in structured datasets, refer to *Data Science: Concepts and Practice* (Kotu, V. and Deshpande, B., 2019).

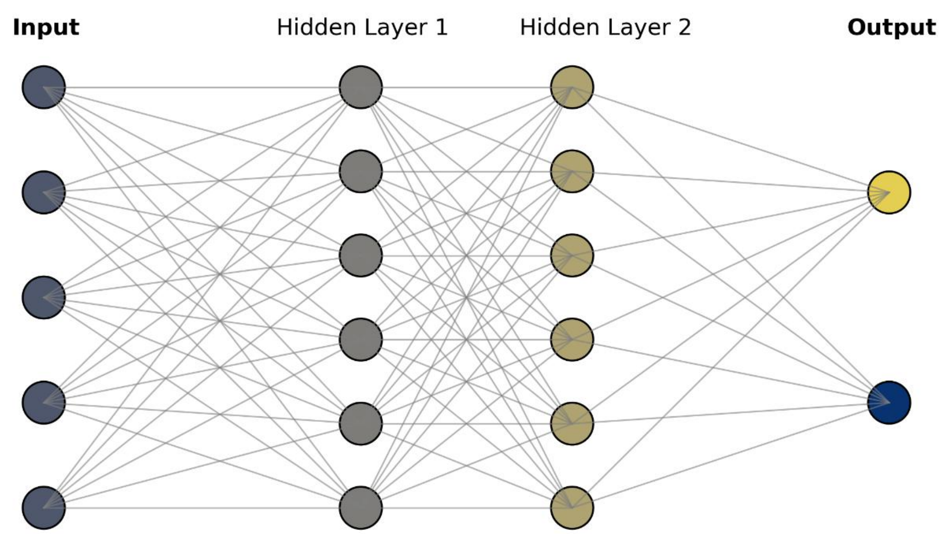

Figure 7: ANN diagram (Author's own).

This diagram illustrates the layered structure of an ANN, depicting the flow of data from the input layer through the hidden layers to the output layer, highlighting the interconnectedness of neurons across layers.

5.4 Residual Networks

Residual Networks, particularly ResNet-50, are designed to mitigate the vanishing gradient problem in deep neural networks by introducing skip connections, which allow gradients to flow directly through the network layers, facilitating the training of very deep architectures. In their seminal paper, "Deep Residual Learning for Image Recognition," He et al. (He, K., Zhang, X., Ren, S. & Sun, J., 2015) introduced this framework, demonstrating that residual networks are easier to optimise and can gain accuracy from considerably increased depth. The ResNet-50 model comprises 50 layers, utilising these residual blocks to enhance feature learning and performance. This architecture has been widely adopted for various image recognition tasks due to its effectiveness in training deep networks.

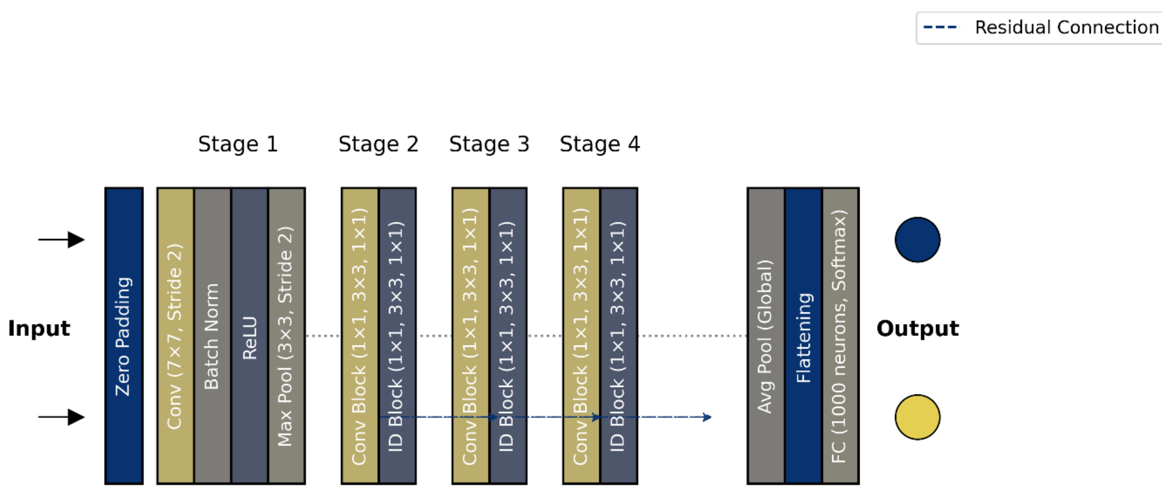

Figure 8: ResNet-50 diagram (Author's own).

This diagram illustrates the layered structure of ResNet-50, highlighting the implementation of skip connections that facilitate the training of deep networks by mitigating issues related to vanishing gradients

5.5 Visual Geometry Group Network

VGGNet, developed by Simonyan and Zisserman (Simonyan, K. & Zisserman, A., 2015), is renowned for its simplicity and effectiveness in image classification tasks. The architecture employs multiple convolutional layers with small receptive fields (3×3), followed by max-pooling layers, enabling deep feature extraction while maintaining computational efficiency. In this study, the pretrained VGG16 model was utilised, wherein the top layers were replaced with custom dense layers to facilitate binary classification. Transfer learning was employed by freezing the base layers of the VGGNet model, thereby retaining generalised features learned from the ImageNet dataset while training the newly added layers on the specific task. The model was trained using the Adam optimiser and categorical cross-entropy loss function, ensuring robust convergence. This approach leverages the depth and simplicity of VGGNet to achieve high performance in image classification tasks. For a detailed discussion on the application of VGGNet in image classification, refer to Simonyan and Zisserman's *Very Deep Convolutional Networks for Large-Scale Image Recognition* (Simonyan, K. & Zisserman, A., 2015).

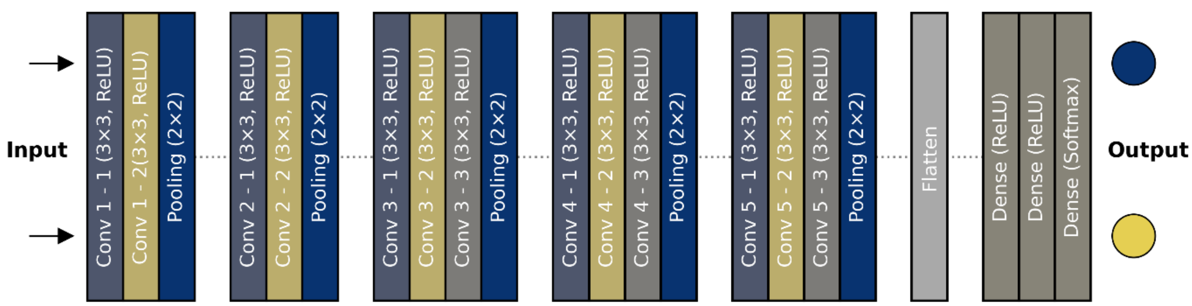

Figure 9: VGGNet16 diagram (Author's own).

This diagram illustrates the sequential arrangement of convolutional and pooling layers in VGGNet, highlighting its deep yet straightforward structure.

5.6 Vision Transformers

Vision Transformers represent a paradigm shift in image processing by applying transformer architectures, traditionally used in natural language processing, directly to image data. Introduced by Dosovitskiy et al. (Dosovitskiy, A., B. Fischer, 2020), ViT models divide an input image into fixed-size patches, typically 16×16 pixels, and flatten each into a one-dimensional vector. These vectors are then linearly embedded and combined with positional embeddings to retain spatial information, forming a sequence akin to token embeddings in text processing. This sequence is fed into a standard transformer encoder composed of multiple layers of multi-head self-attention and feed-forward neural networks, enabling the model to capture global relationships across the entire image. Notably, ViT eliminates the need for convolutional layers, differing from traditional convolutional neural networks (CNNs) by focusing on global context rather than local features. In this study, the ViT model was trained from scratch using the Adam optimiser and sparse categorical cross-entropy loss function. Normalisation techniques were applied to ensure stable training, and early stopping was implemented to prevent overfitting, which is crucial given the model's complexity and the extensive data requirements for effective training. Dosovitskiy et al. (Dosovitskiy, A., B. Fischer, 2020) provide a comprehensive analysis of this model in their paper "An Image is Worth 16x16 Words: Transformers for Image Recognition at Scale," demonstrating that ViT can achieve performance comparable to or surpassing state-of-the-art CNNs when trained on sufficient data.

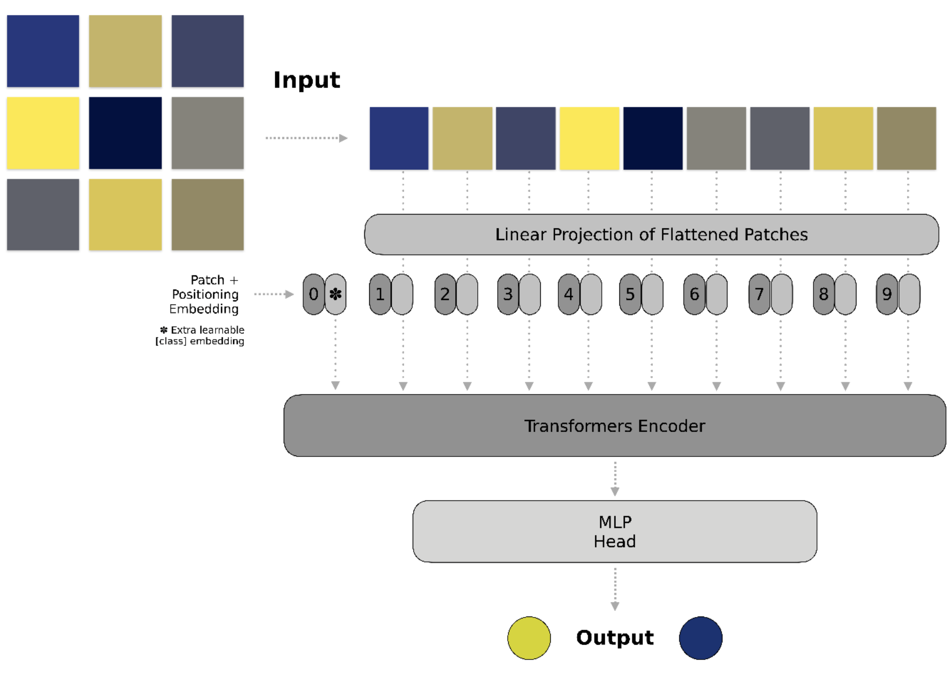

Figure 10: ViT diagram (Author's own).

This diagram illustrates the process of dividing an image into patches, embedding them, and processing through the transformer encoder to achieve image classification.

5.7 Training Parameters and Methodology

To ensure fair comparisons, all models were trained with identical hyperparameters. Training was conducted for up to 60 epochs with a batch size of 64. Early stopping was implemented, halting training after five epochs of no improvement in validation loss. This standardised methodology adheres to machine learning best practices, ensuring consistent and unbiased evaluations across all models.

All figures were generated using *Notebook.ipynb* (2025), except where noted. The Cividis colour palette, designed for enhanced readability and accessibility, was applied to ensure clarity, including for individuals with colour vision variations.

6. Evaluation

Evaluation metrics, including confusion matrices, accuracy, precision, recall, and F1-score, assessed CNN, ANN, ResNet50, VGGNet16 and ViT performance in classifying MRI images for Alzheimer's (Provost, F. and Fawcett, T., 2013).

6.1. Metrics Overview

- The **confusion matrix** is a crucial evaluation tool in machine learning and statistics for binary classification problems. It helps summarise the performance of a classification model by comparing the actual outcomes with the predicted outcomes. Here's how the confusion matrix is organised and interpreted:

		Predicted condition	
	Total Population = P + N	Positive (PP)	Negative (PN)
Actual condition	Positive (P)	True Positive (TP)	False Negative (FN)
	Negative (N)	False Positive (FP)	True Negative (TN)

Figure 11: Confusion matrix structure (Author's own).

    - True Positives: Correct positives.
    - True Negatives: Correct negatives.
    - False Positives: Incorrect positives.
    - False Negatives: Missed positives.

- **Accuracy:** Measures overall correctness:
  Accuracy = TP + TN / TP + TN + FP + FN
  Accuracy alone can mislead with imbalanced datasets, requiring additional metrics.

- **Precision:** Assesses correct positive predictions:
  Precision = TP / TP + FP
  High precision minimises false positives and unnecessary treatments.

- **Recall:** Captures the ability to detect positives:
  Recall = TP / TP + FN
  High recall reduces missed diagnoses, crucial for Alzheimer's.

- **F1-Score:** Balances precision and recall:
  F1-Score = 2· (Precision · Recall) / (Precision + Recall)

6.2. Evaluation of CNN

The Convolutional Neural Network model exhibited strong classification performance, as evidenced by accuracy, loss, and confusion matrix results.

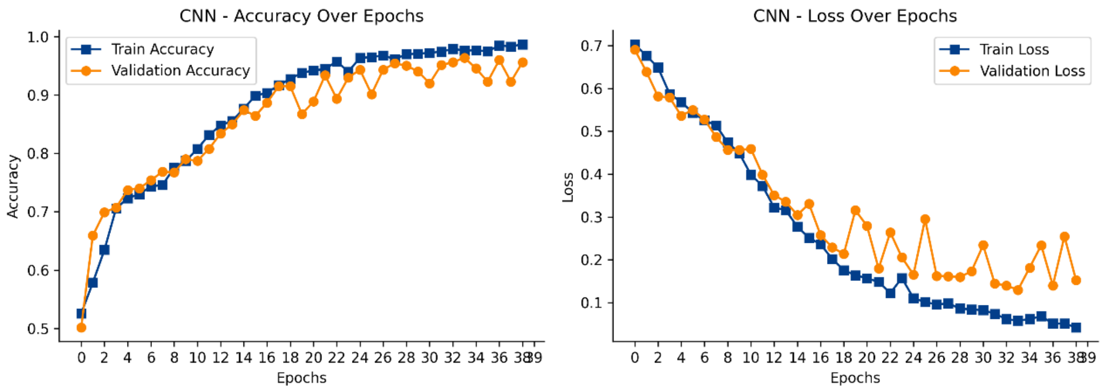

Figure 12: CNN accuracy and loss.

Figure 12 illustrates accuracy and loss curves over epochs, showing a steady rise in both training and validation accuracy. The training accuracy peaked at 98.67%, while validation accuracy stabilised at 95.61%, with minor fluctuations. The loss curve shows a consistent drop in training loss, whereas validation loss initially decreases before fluctuating, indicating variability in model performance across validation samples.

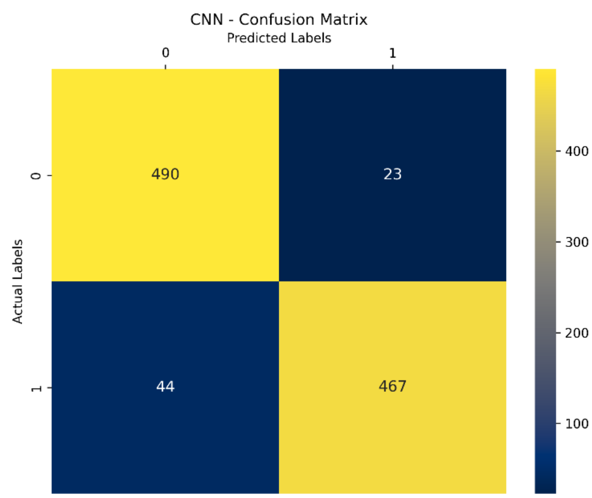

Figure 13: CNN confusion matrix.

Figure 13, the confusion matrix, reveals that the model accurately classified 490 instances of class 0 and 467 of class 1, with 23 false positives and 44 false negatives, suggesting a slight imbalance. The test accuracy of 93.46% confirms the model's effectiveness in distinguishing categories. The classification report supports these findings, highlighting high precision, recall, and F1-scores for both classes, albeit with slight variations.

6.3. Evaluation of ANN

The Artificial Neural Network model demonstrated strong classification performance, as shown in accuracy, loss, and confusion matrix results.

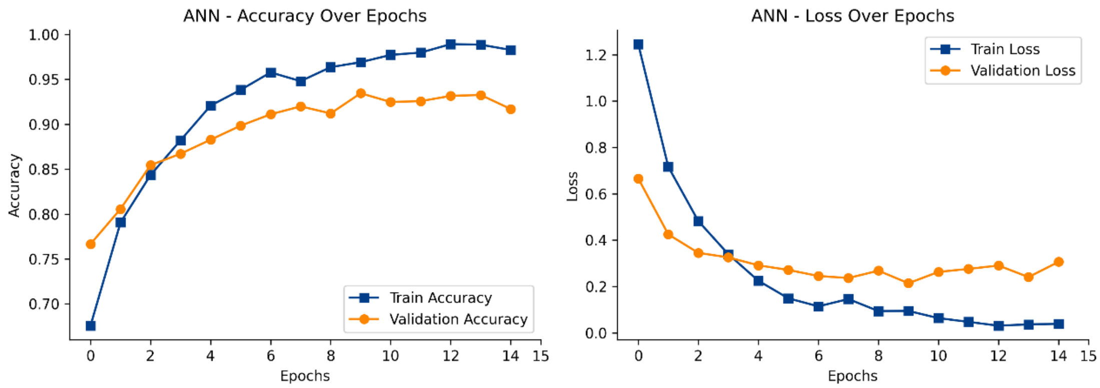

Figure 14: ANN accuracy and loss.

Figure 4 illustrates accuracy and loss trends over epochs, where training accuracy steadily improved, reaching 98.28%, while validation accuracy peaked at 91.70%. The validation accuracy followed a similar pattern to training accuracy but exhibited fluctuations, especially in later epochs. The loss curve in Figure 14 shows a consistent decline in training loss, whereas validation loss initially decreased before fluctuating, suggesting some variability in model generalisation.

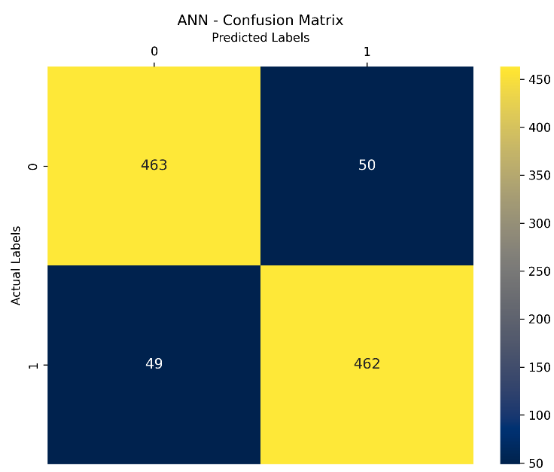

Figure 15: ANN confusion matrix.

Figure 15, the confusion matrix, further highlights classification performance, with the ANN correctly classifying 463 instances of class 0 and 462 of class 1. Misclassifications included 50 false positives and 49 false negatives, indicating a relatively balanced performance across both classes. The overall test accuracy of 90.10% confirms the model's effectiveness. The classification report supports these findings, with high precision, recall, and F1-scores, averaging 90% across all metrics.

6.4. Evaluation of ResNet50

The ResNet50 model exhibited moderate classification performance, as reflected in accuracy, loss, and confusion matrix results.

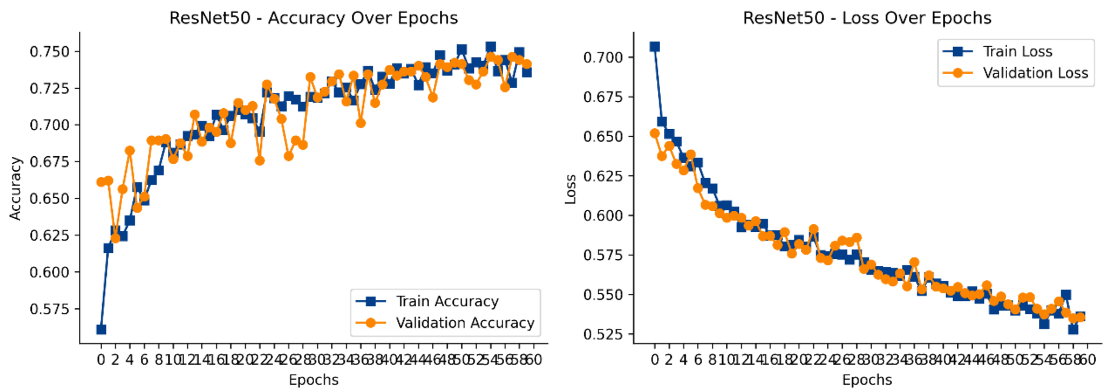

Figure 16: ResNet50 accuracy and loss.

Figure 16 shows accuracy and loss trends over epochs, with training and validation accuracy steadily increasing to 73.57% and 74.12%, respectively. Both curves follow a similar pattern, though frequent fluctuations indicate variability in learning. The loss curve shows a consistent decline, with validation loss stabilising at 0.5357, suggesting a gradual learning process without significant overfitting.

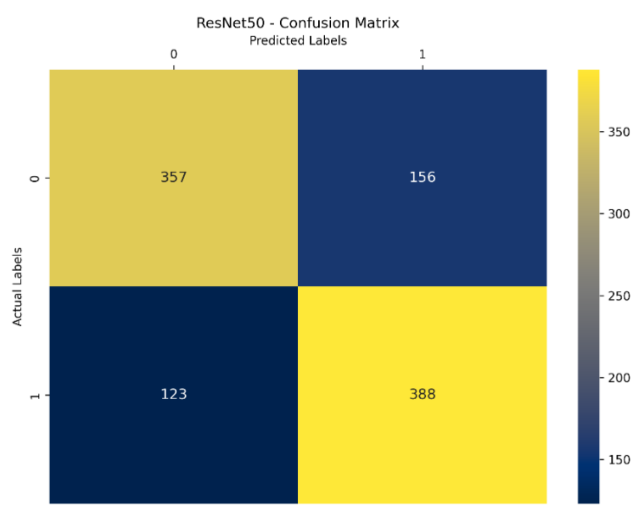

Figure 17: ResNet50 confusion matrix.

Figure 17, the confusion matrix, provides further classification insights. The model correctly classified 357 instances of class 0 and 388 of class 1, while misclassifications included 156 false positives and 123 false negatives, indicating some class imbalance. The overall test accuracy of 72.75% confirms moderate classification performance. Precision, recall, and F1-scores hover around 73% for both classes, showing that while ResNet50 captures dataset patterns, its performance remains variable across different samples.

6.5. Evaluation of VGGNet16

The VGGNet16 model demonstrated strong classification performance, as evidenced by accuracy, loss, and confusion matrix results.

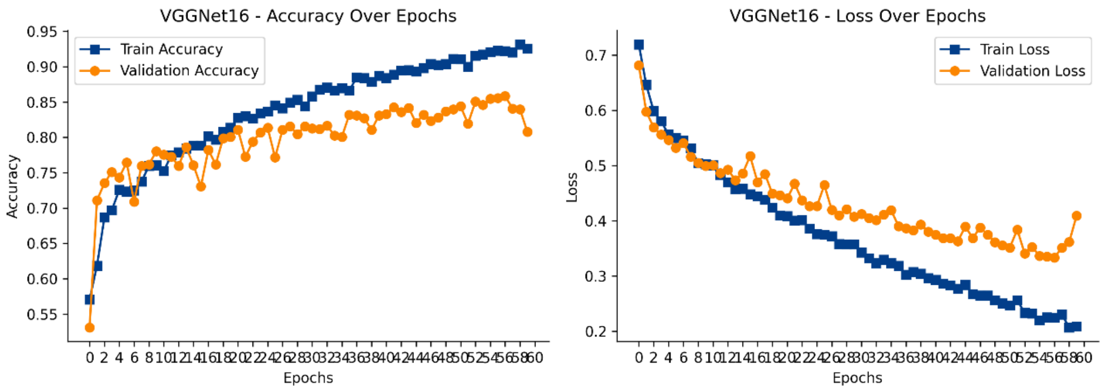

Figure 18: VGGNet16 accuracy and loss.

Figure 18 illustrates accuracy and loss trends over epochs, with training accuracy steadily increasing to 92.53% and validation accuracy stabilising at 80.76%. While validation accuracy follows a similar trend to training accuracy, minor fluctuations occur, especially in later epochs. The loss curve shows a consistent decline in training loss, while validation loss initially decreases but fluctuates later, indicating some variability in generalisation.

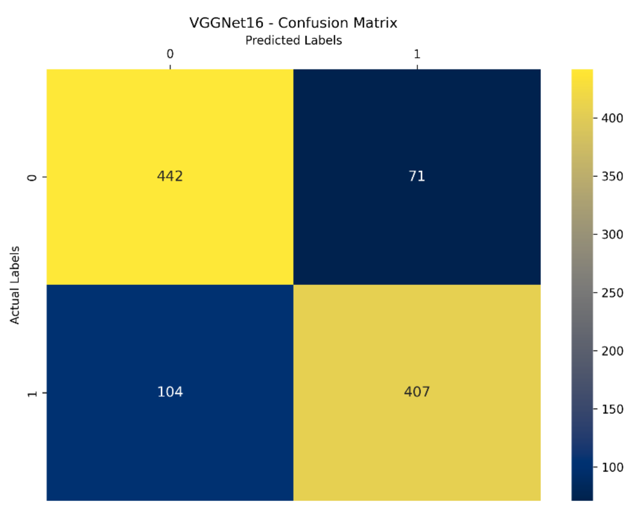

Figure 19: VGGNet16 confusion matrix.

Figure 19, the confusion matrix, further supports the model's classification performance. The model correctly identified 442 instances of class 0 and 407 of class 1, with 71 false positives and 104 false negatives, suggesting a slightly higher misclassification rate for class 1. The overall test accuracy of 82.91% confirms its effectiveness. The classification report highlights high precision, recall, and F1-scores, averaging 83%, demonstrating VGGNet16's reliability in capturing dataset patterns.

6.6. Evaluation of ViT

The Vision Transformer model exhibited strong classification performance, as reflected in accuracy, loss, and confusion matrix results.

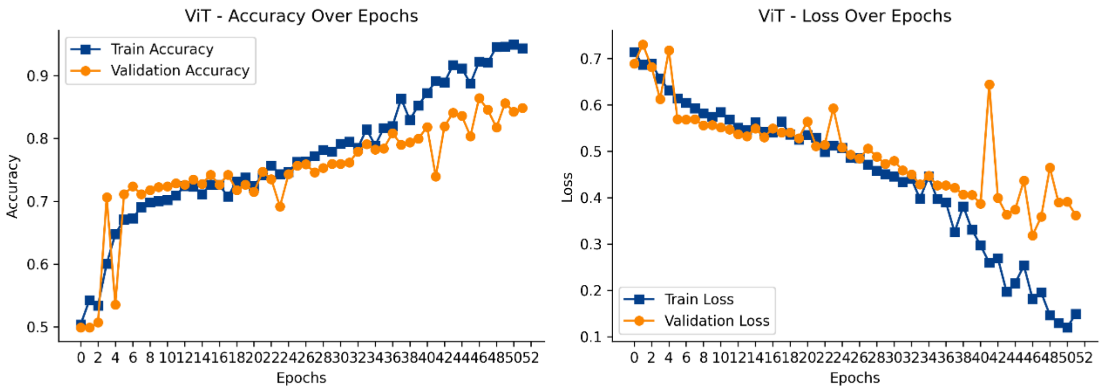

Figure 20: ViT accuracy and loss.

Figure 20 presents accuracy and loss trends over epochs, showing a steady increase in both training and validation accuracy, reaching 87.04% and stabilising at 86.23%, respectively. Validation accuracy follows a similar pattern to training accuracy but fluctuates slightly, particularly in later epochs. The loss curve shows a consistent decline in training loss, while validation loss initially decreases but fluctuates before stabilising, indicating some variability in generalisation.

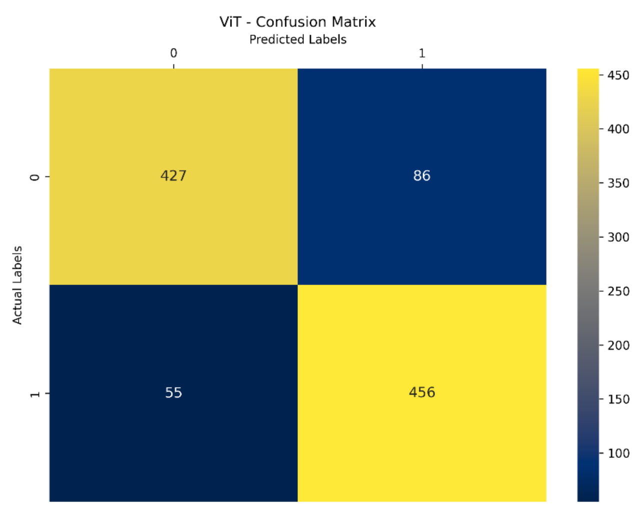

Figure 21: ViT confusion matrix.

Figure 21, the confusion matrix, further illustrates classification performance, with the model correctly classifying 427 instances of class 0 and 456 of class 1. Misclassifications included 86 false positives and 55 false negatives, suggesting a slightly higher error rate for class 0. The test accuracy of 86.23% confirms the model's reliability, supported by high precision, recall, and F1-scores, averaging 86% across all metrics.

6.7. Evaluation and Comparison of Model Performances

The comparative evaluation of the five models - CNN, ANN, ResNet50, VGGNet16, and ViT - is summarised in Figure 22 and Figure 23, showcasing key performance metrics, including accuracy, precision, recall, F1-score, and classification outcomes (Provost, F. and Fawcett, T., 2013).

Metric	CNN	ANN	ResNet50	VGGNet16	ViT
Accuracy	0.93	0.90	0.73	0.83	0.86
Precision	0.94	0.90	0.73	0.83	0.86
Recall	0.93	0.90	0.73	0.83	0.86
F1 Score	0.93	0.90	0.73	0.83	0.86
True Positive	467	462	388	407	456
True Negative	490	463	357	442	427
False Positive	23	50	156	71	86
False Negative	44	49	123	104	55

Figure 22: Model performance comparison (Author's own).

In Figure 22, CNN achieves the highest accuracy (0.93), followed closely by ANN (0.90) and ViT (0.86). VGGNet16 ranks next with 0.83, while ResNet50 performs the worst (0.73). Precision, recall, and F1-score follow a similar trend, with CNN leading (0.94, 0.93, 0.93) and ResNet50 showing the lowest scores (0.73 for all three metrics). The true positive and true negative counts further validate this ranking, where CNN correctly classified 467 positive and 490 negative cases, while ViT, ANN, and VGGNet16 also performed well, though with slightly higher misclassification rates. ResNet50 had the highest errors, recording 156 false positives and 123 false negatives, highlighting its weaker classification performance and struggles in distinguishing between the two classes.

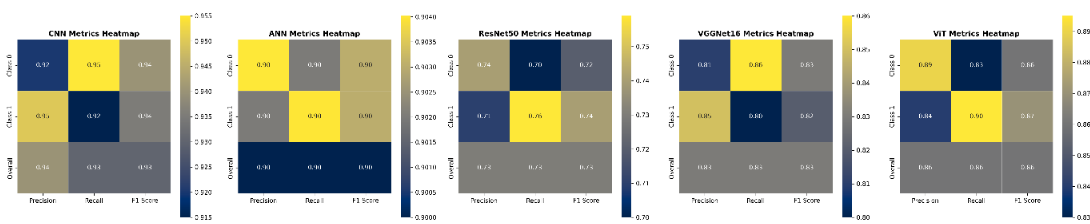

Figure 23: Precision, recall, and F1-score heatmaps (Author's own).

Figure 23 provides a more granular view of class-wise metrics. CNN and ANN show the most balanced performance across both classes, with high recall and precision values, making them the most stable models. ViT also performs well, with an F1-score of 0.86, indicating strong classification capabilities. VGGNet16 follows closely, maintaining reasonable accuracy, while ResNet50 exhibits the weakest classification performance, particularly in false positive and false negative rates. Overall, CNN emerges as the best-performing model, demonstrating the highest reliability, precision, and classification accuracy. ANN follows as the second-best, with ViT ranking third due to slightly lower accuracy but still performing effectively. VGGNet16 remains competitive, while ResNet50 lags significantly, with the lowest accuracy and highest misclassification.

7. Deployment

In this project, the selected deep learning model, Convolutional Neural Networks (CNN), demonstrated the highest classification accuracy for Alzheimer's detection using MRI scans. The model is deployed as a cloud-based application, integrating with healthcare systems for seamless diagnosis and monitoring.

To ensure usability, a web-based interface is developed where radiologists and clinicians can upload MRI scans for automated classification. The model is hosted on a cloud server using TensorFlow Serving, providing real-time predictions via an API. Security measures, such as encryption and access control, safeguard patient data. The deployment strategy also includes continuous model monitoring to ensure performance consistency, with periodic retraining using updated datasets to maintain accuracy and reliability.

Post-deployment, feedback from medical professionals is collected to refine the system further. The integration of AI-driven diagnostics into clinical workflows is expected to assist in early Alzheimer's detection, supporting timely intervention and improving patient outcomes.

8. Future Work

Future improvements will focus on enhancing model performance and expanding its applicability. AI-driven medical imaging advancements can improve diagnostic accuracy by generating ultra-high-resolution scans from lower-resolution images, enabling more precise analysis (UCSF, 2024).

Additionally, AI can facilitate early disease detection by identifying subtle patterns across thousands of images, allowing for timely interventions and improved patient outcomes. Further collaboration with healthcare institutions will ensure regulatory compliance and clinical validation.

Continuous refinement of explainable AI (XAI) methods will enhance trust among medical professionals, fostering widespread adoption. Ultimately, integrating AI-powered diagnostics into broader healthcare frameworks will drive efficiency and accessibility in medical imaging (UCSF, 2024).

9. References

BorhaniTrash, A., 2021. *Alzheimer MRI Disease Classification [Dataset].* [Online]
Available at: https://www.kaggle.com
[Accessed 20 May 2025].

Dosovitskiy, A., B. Fischer, 2020. *An image is worth 16x16 words: Transformers for image recognition at scale.* Vancouver, Canada, Proceedings of the NeurIPS 2020 Conference.

Goodfellow, I., Bengio, Y., and Courville, A. , 2016. *Deep Learning.* s.l.:MIT Press.

He, K., Zhang, X., Ren, S. & Sun, J., 2015. *Deep Residual Learning for Image Recognition.* [Online]
Available at: https://arxiv.org/abs/1512.03385
[Accessed 20 May 2025].

Kotu, V. and Deshpande, B., 2019. Chapter 10. In: M. Kaufmann, ed. *Data Science: Concepts and Practice..* Amsterdam: 2nd ed., pp. 307 - 342.

McRobbie, D.W., Moore, E.A., Graves, M.J., & Prince M.R., 2017. *MRI from Picture to Proton.* 3rd ed ed. Cambridge: Cambridge University Press.

Ng, A., 2018. *Machine Learning Yearning: Technical Strategy for AI Engineers.* s.l.: Deeplearning.AI.

Provost, F. and Fawcett, T., 2013. *Data science for business: what you need to know about data mining and data-analytic thinking.* 1st ed., 2nd release ed. Beijing and Cologne: O'Reilly.

Simonyan, K. & Zisserman, A., 2015. *Very deep convolutional networks for large-scale image recognition.* Lille, France, Proceedings of the International Conference on Machine Learning.

UCSF, 2024. *4 ways artificial intelligence is poised to transform medicine.* [Online]
Available at: https://www.ucsf.edu/news/2024/12/429031/4-ways-artificial-intelligence-poised-transform-medicine
[Accessed 20 May 2025].

WHO, 2023. *Dementia: Key Facts.* [Online]
Available at: https://www.who.int
[Accessed 20 May 2025].